# Vibration Parameter Optimization of a Linear Vibrating Banana Screen Using DEM 3D Simulation

**Xiaoqiu Wu[1], Zhanfu Li[2], Huihuang Xia[1] & Xin Tong[1,*]**

[1]School of Mechanical Engineering and Automation,
Huaqiao University, Jimei Avenue, Xiamen 361021, China
[2]School of Mechanical and Automobile Engineering,
Fujian University of Technology, South Xuefu Road, Fuzhou 350118, China
[*]E-mail: xtong@fjut.edu.cn

**Abstract.** In this paper, the effects of vibration parameters of a banana screen, i.e. frequency, amplitude and vibration direction angle, on the screening efficiency per unit time were studied using the discrete element method (DEM). The simulations were validated according to data collected from an experimental prototype screen. Functional relationships between vibration parameters and screening efficiency per unit time are presented. The results showed that the screening efficiency per unit time first displays an increase and later a decrease when the frequency, amplitude or vibration direction angle increased respectively. Vibration parameter optimization was also investigated, using an orthogonal experiment. Based on the banana screen model, it can be concluded that when the frequency is 22 Hz, the amplitude is 2.2 mm and the vibration direction angle is 39°, the screening efficiency of a banana screen is optimal.

**Keywords**: *banana screen; DEM simulation; optimization; screening efficiency per unit time; vibration parameter.*

## 1 Introduction

Screening, one of the oldest and most diffusely applied physical size separation approaches [1], is a process that refers to enabling a mixture of particles of different sizes to pass a working surface with a certain number of apertures to achieve size classification. It is extensively employed in industries, ranging from traditional mineral, metallurgical, chemical, food, pharmaceutical to sanitation sectors. The vibrating screen is one of the most commonly used screening devices in manufacture [2]. The banana screen, a particularly designed vibrating screen where the slopes of the screen deck change from steep at the feed end to flat at the discharge end in order to maintain a constant bed thickness [3], is widely used in industry on account of its higher efficiency and larger capacity compared to ordinary vibrating screens [4].

To achieve further enhancements on sieving efficiency and capacity, some researchers have studied factors that are able to affect the screening results. For

Received June 20th, 2017, 1st Revision March 29th, 2018, 2nd Revision May 15th, 2018, Accepted for publication August 13th, 2018.
 ISSN: 2337-5779, DOI: 10.5614/j.eng.technol.sci.2018.50.3.3

ordinary linear vibrating screens, the effect of screen length on the screening efficiency of particles has been studied under various single parameter conditions, including frequency, amplitude, vibration angle and screen inclination [5]. For swing vibrating screens, the efficiency of particle screening has been investigated at different values of frequency and swing declination angle [2]. For banana screens, the motion characteristics and penetrating mechanisms of the particles on the screen deck have been studied and the effects of geometric parameters such as the inclination and deck length have also been discussed [4]. The particle flow in typical multi-deck banana screens has been numerically simulated and the impacts of vibration conditions and geometry of the screen on the sieving processes have been studied [3]. However, with regard to the relationship between parameters and screening performance of banana screens, more research still needs to be done.

The discrete element method (DEM) is a numerical method capable of describing the mechanical behavior of assemblies of discs and spheres and has been proved to be appropriate for simulating the process of sieving with particles in large quantities based on the particles' motion on the screen and the interactions between the particles or between the particles and the screen plate [6]. It has already been used to perform batch and continuous screening investigations with varying particle characteristics and sieving parameters [7]. Cleary and Sawley [8] adopted DEM to capture spherical particles on an inclined flat sieve. Besides, simulation of particle stratification and penetration of a linear vibrating screen has been performed to analyze the influence of a range of structural parameters [9]. Also, DEM played a crucial role in researches on mineral screening and crop cleaning [10-13]. In addition, because DEM can be used as an effective tool to design new facilities long before a prototype is even fabricated [14], it is also commonly used in many other fields.

In this paper, a three-dimensional DEM simulation study of a banana screen with 5 decks is presented that was conducted to probe the influence of vibration parameters on linear sieving performance. This was evaluated by screening efficiency per unit time using a single factor experiment. Moreover, an orthogonal experimental design was applied to compare the extent of influence of each vibration parameter and to obtain the optimal combination of parameters for achieving the highest screening efficiency.

## 2 Mathematical Model

### 2.1 Discrete Element Method

DEM is a practical tool and is widely used in many areas of industrial production [15-17]. According to the interactions between rigid bodies during

the process of collision, DEM can trace the motions of individual particles accurately based on Newton's second law of motion. The translational and rotational motions of a particle (*i*) can be deduced as follows:

$$m_i \frac{d^2 x_i}{dt^2} = \sum_{j=1}^{n_i} (F_{cn,ij} + F_{ct,ij} + F_{dn,ij} + F_{dt,ij}) + m_i g \tag{1}$$

$$I_i \frac{d\theta_i}{dt} = \sum_{j=1}^{n_i} (T_{ij} + M_{ij}) \tag{2}$$

where $m_i$, $I_i$, $x_i$ and $\theta_i$ are the mass, the moment of inertia, the translational and angular velocities of particle *i*, respectively; $g$ is the gravitational acceleration; $F_{cn,ij}$ and $F_{ct,ij}$ are the normal and tangential forces; $F_{dn,ij}$ and $F_{dt,ij}$ are the normal and tangential damping forces; $T_{ij}$ and $M_{ij}$ are the torques caused by rolling friction and tangential forces.

This specific contact model is based on the work of Mindlin and Deresiewicz [18]. The normal force, $F_{cn,ij}$, which appears in Eq. (1), is given by Eq. (3) as follows:

$$F_{cn,ij} = \frac{4}{3} E^* \sqrt{R^*} \delta_n^{3/2} \tag{3}$$

where $E^*$ is the equivalent Young's modulus; $R^*$ is the equivalent radius; $\delta_n$ is the normal overlap. And the normal damping force, $F_{ct,ij}$, is given by Eq. (4) as follows:

$$F_{dn,ij} = -2\sqrt{\frac{5}{6}} \xi \sqrt{k_n m^*} v_n^r \tag{4}$$

where $m^*$ is the equivalent mass; $\xi$ is the critical damping coefficient; $k_n$ is the normal stiffness; $v_n^r$ is the normal component of the relative velocity. Additionally, the tangential force and tangential damping force can usually be calculated with Eqs. (5) and (6) as follow:

$$F_{ct,ij} = -k_t \delta_t \tag{5}$$

$$F_{dt,ij} = -2\sqrt{\frac{5}{6}} \xi \sqrt{k_t m^*} v_t^r \tag{6}$$

where $k_t$ is the tangential stiffness; $\delta_t$ is the tangential overlap; $v_t^r$ is the tangential component of the relative velocity. Besides the abovementioned forces, the torques are given by Eqs. (7) and (8) as follows:

$$T_{ij} = -\mu_r F_{cn,ij} R_i \hat{\theta} \tag{7}$$

$$M_{ij} = R_i \times (F_{ct,ij} + F_{dt,ij}) \tag{8}$$

where $\mu_r$ is the coefficient of the rolling friction; $R_i$ is the distance between the center of mass and the contact point; $\hat{\theta}$ is the unit angular velocity vector of the object at the contact point.

## 2.2 EDEM Software

EDEM is a CAE software application based on DEM that is widely used to perform simulations and analyses of the movement process of particle flow in various production operations. EDEM can be divided into three parts: Creator, Simulator, and Analyst. It can simulate and trace all kinds of particle motions excellently. Also, it can give microscopic information of the particles at a certain time during the process of the particles moving. Therefore, EDEM was used to simulate the screening process of a banana screen in this study.

# 3 Simulation and Experiment

## 3.1 Particle Shapes Applied in the Simulations

In DEM, particles are traditionally approximated by discs or spheres, in two and three dimensions respectively, on account of the high computational efficiency of these shapes [14]. However, these shapes are usually too ideal compared to real particle shapes in nature. As a result, the quantitative predictive accuracy of the simulation will be degraded to some extent. Researches have been conducted to overcome this disadvantage. For instance, elliptical particles have been used to explore shape effects [19], while polygonal particles have been applied to represent rocks and sea ice blocks [20-21]. Additionally, Potapov and Campbell have used bonded assemblies of polygonal particles to model brittle fracture during impact [22].

In order to reduce the influence of particle shapes on the result of the simulation, the particles applied in this work were averagely divided into six kinds of different typical shapes, as displayed in Figure 1. These particles with different shapes were created by gluing identical spherical particles together to make simple non-spherical shapes with a clustering approach. The virtual

diameter of a non-spherical particle was defined as the diameter of a sphere whose volume is equal to the non-spherical one [23]. The computational formula of the virtual diameter is:

$$d_V = (\frac{6V}{\pi})^{\frac{1}{3}} \tag{9}$$

where $d_V$ is the virtual diameter of a non-spherical particle (mm), $V$ is the volume of a complex shaped particle ($mm^3$).

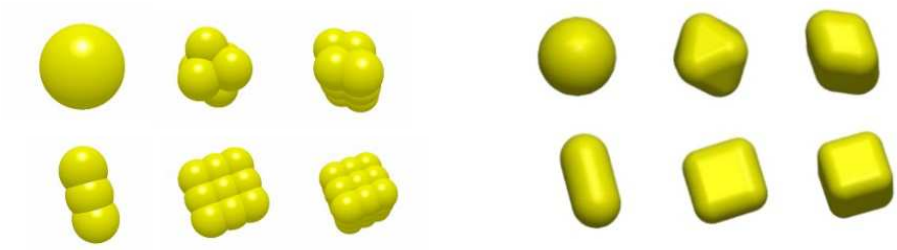

(a) (b)

**Figure 1** Six kinds of typical shapes applied in the simulations.

## 3.2 Simulation Conditions

In this research, a banana screen with five decks was employed, where the angle difference of each pair of neighboring decks was 5.5° (see Figure 2). A three-dimensional DEM screening simulation was conducted as shown in Figure 3. In addition, the inclination of the third deck was invariably 14°, while the banana surface oscillated in a straight line. Particles of different diameters produced and stored in a particle factory dropped out from the hopper by gravity, then collided with the vibrating screen decks and finally penetrated through the banana screen or reached the discharge end.

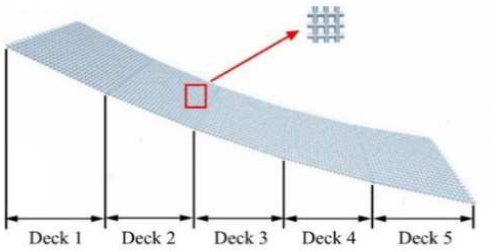


**Figure 2** Diagrammatic sketch of banana screen deck.

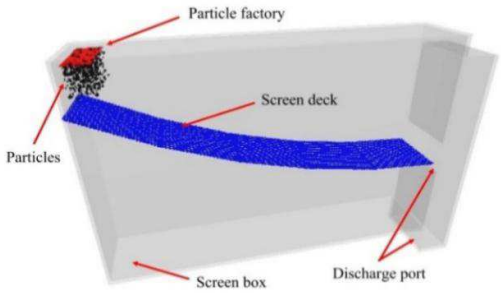


**Figure 3** Diagrammatic sketch of vibrating banana screen model.

The effects of vibration parameters, i.e. frequency, amplitude and vibration direction angle, on the banana screen were studied by a single factor experiment. The detailed parameters and simulation conditions are listed in Table 1.

**Table 1** List of simulation parameters.

| **Material properties** | **Poisson's ratio** | **Shear modulus** | **Density** |
|---|---|---|---|
| Particle | 0.3 | 23 Mpa | $2678\,kg/m^3$ |
| Deck/box | 0.29 | 79980 Mpa | $7861\,kg/m^3$ |
| Collision properties | Restitution coefficient | Static friction | Rolling friction |
| Inter-particle | 0.1 | 0.545 | 0.01 |
| Particle-deck | 0.2 | 0.5 | 0.01 |
| Particle diameter | Mean 0.5 and 1.0 mm; SD: 0.55 | | |
| Particle generate rate | 1666 particles/s | | |
| Total particle number | 10000 | | |
| Screen length (mm) | 160 in horizontal projection | | |
| Screen width (mm) | 30 | | |
| Wire diameter (mm) | 0.7 | | |
| Aperture size (mm) | $0.7 \times 0.7$ | | |
| Frequency (Hz) | 15,20,25,30,35,40 | | |
| Amplitude (mm) | 1.5,2,2.5,3,3.5,4,4.5 | | |
| Vibration direction angle (°) | 25,30,35,40,45,50,55 | | |

## 3.3 Screening Efficiency per Unit Time

The aim of screening is to obtain particles of specific sizes from many different mixed materials. Therefore, the screening efficiency per unit time is proposed in this paper to act as an evaluation indicator of sieving performance. We chose particles with a diameter of 0.7 mm and 0.6 mm respectively to be the target particles and the screening efficiency per unit time used in this paper is given by Eq. (10)[2]:

$$\eta = \frac{\left(\frac{M_{S1}}{M_{S2}} - \frac{M_{L1}}{M_{L2}}\right) \times 100\%}{t} \tag{10}$$

where $\eta$ is the screening efficiency per unit time (%/s); $M_{S1}$ is the mass of particles whose diameters are smaller than the target particle size in the undersized material (kg); $M_{S2}$ is the total mass of particles whose diameters are smaller than the target size (kg); $M_{L1}$ is the mass of particles whose diameters are larger than the target size in the undersized material (kg); $M_{L2}$ is the total mass of particles whose diameters are larger than the target size (kg); $t$ is the duration of the sieving process ($s$).

## 3.4 Results and Discussion

### 3.4.1 Effects of Vibration Frequency

Vibration frequency has a significant impact on the bouncing performance of granular materials on a screen. At low frequency, particulate materials move slowly and it takes a relatively long time for all particles to complete the screening process and as a result the screening efficiency per unit time is low. However, a high frequency may cause severe vibration, which reduces the contact between particles and the screen deck and a low screening efficiency per unit time is achieved.

Figure 4 presents the simulation results on the effects of vibration frequency on screening efficiency per unit time at a fixed amplitude of 2 mm and a fixed direction angle of 45°. The squares and circles in Figure 4 stand for the data points whose target particle diameters are 0.7 mm or 0.6 mm respectively. The graph demonstrates that the efficiency of distinct particle diameters promptly increased with growing frequency when the frequency was under 20 Hz and decreased comparatively slowly when the frequency was over 20 Hz. This means that the value of 20 Hz may be the optimum frequency for screening efficiency per unit time on the investigated banana screen.

According to the data points in Figure 4, the relationship between screening efficiency per unit time and frequency can be fitted by the function shown in Eq. (11) with very small fitting errors (RelE in Figure 4). The black and red lines in Figure 4 are the fitting curves.

$$y = (a + bx + cx^2 + dx^3)e^{-px} \tag{11}$$

where $y$ is the screening efficiency per unit time (%/s); $x$ is the vibration frequency (Hz); $a$, $b$, $c$, $d$ and $p$ are the correlation coefficients of the respective particle size.

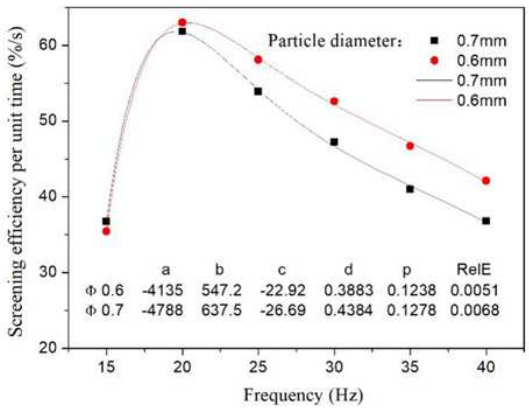


**Figure 4** Influence of frequency on screening efficiency per unit time.

### 3.4.2 Effects of Vibration Amplitude

Vibration amplitude can provide particulate materials with energy for transportation. The looseness and penetration will be not reasonable for particles when the amplitude is too low or too high, which will result in low screening efficiency with increased processing time.

Figure 5 shows how the screening efficiency per unit time depends on the vibration amplitude for particles of different diameters when the values of frequency and direction angle are 20 Hz and 45°. The efficiency first displays an increasing and later a decreasing trend along with the increase of the amplitude. When the amplitude is 2 mm, the value of the efficiency will reach its maximum, which means 2 mm is likely to be the optimal amplitude for improving sieving efficiency.

The data points obtained from these simulations can be fitted to smoothen the curve with the formula in Eq. (12):

$$y = \frac{a}{x^3} e^{-\frac{b}{x^3}} + c \tag{12}$$

where $y$ is the screening efficiency per unit time (%/s); $x$ is the vibration amplitude (mm); $a$, $b$ and $c$ are the fitted relation coefficients depending on the diameter of the particles.

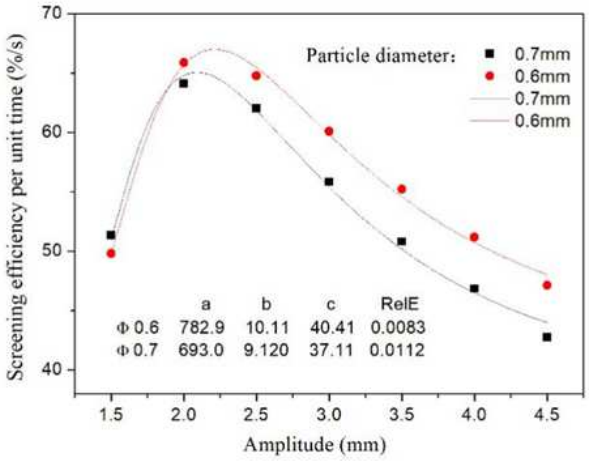


**Figure 5** Influence of amplitude on screening efficiency per unit time.

### 3.4.3 Effects of Vibration Direction Angle

The vibration direction angle affects material transport in a similar way as the amplitude does. Therefore, they have a similar impact on the screening efficiency per unit time.

Figure 6 reveals how the vibration direction angle acting on the banana screen affects the screening efficiency per unit time at an unaltered frequency of 20 Hz and a fixed amplitude of 2 mm. It indicates that the vibration direction angle generates peak efficiency when the direction angle is 35° for particles of different sizes. However, the efficiency diminishes when the direction angle is higher or lower than this point. Hence, approximately 35° is the best choice for the vibration direction angle in view of screening efficiency per unit time.

In the same way, a mathematical relationship between vibration direction angle and screening efficiency per unit time was set up in Eq.(13) as follows:

$$y = (a + \frac{b}{x^2})e^{-\frac{c}{x}} \tag{13}$$

where $y$ is the screening efficiency per unit time (%/s); $x$ is the vibration direction angle (°); $a$, $b$ and $c$ are the mathematical parameters lying on the particle size.

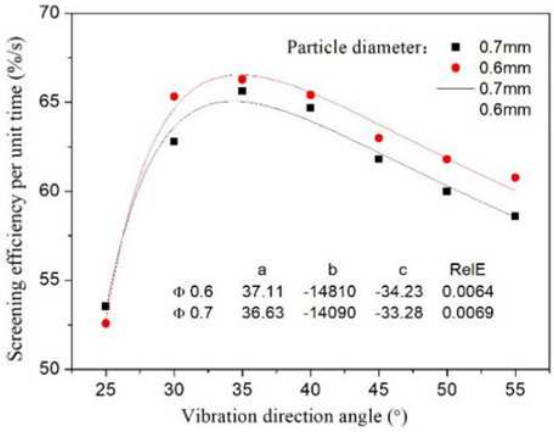


**Figure 6** Influence of vibration direction angle on screening efficiency per unit time.

## 3.5 Experimental Verification

In order to prove the reliability of the simulation results, a series of experiments was conducted so that the real results could be compared with the simulation results. Figure 7 presents the prototype of the vibrating banana screen that was used in the experiment. Several sieving experiments to investigate vibration and structure parameters have already been performed with this prototype [5]. In this validation test, three vibration parameters, i.e. frequency, amplitude and vibration direction angle, were studied; the experimental conditions are listed in Table 2. Other screening parameters, i.e. wire diameter, aperture size and so on, kept the same setting as in the simulations.

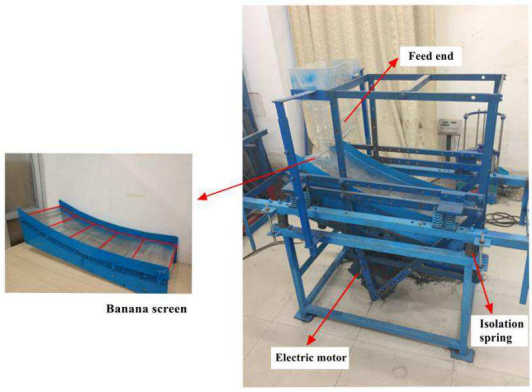


**Figure 7** Experimental prototype of vibrating banana screen.

**Table 2** Experimental conditions.

| Experiments | Vibration parameters | | |
|---|---|---|---|
| | Frequency (Hz) | Amplitude (mm) | Vibration direction angle (°) |
| First group | 15,20,25,30,35 | 20 | 45 |
| Second group | 2 | 1.5,2.0,2.5,3.0,3.5 | 45 |
| Third group | 2 | 20 | 25,35,45,55 |

Sand was chosen to serve as the experimental raw material. For the sake of the acquisition of the different particle sizes that were divided in the simulation, a shock type-based vibrating screen (see Figure 8) was employed to sieve materials of different sizes (D refers to the aperture size of each screen mesh in Figure 8).


**Figure 8** Shock type-based vibrating screen.

Figures 9-11 respectively show a comparison of the DEM simulations and the experiment on frequency, amplitude and vibration direction angle of the banana screen. It is obvious that it is very difficult to cover every particular factor precisely in a simulation model [24]. Firstly, the parallels of material properties, collision properties as well as input settings between numerical simulations and a real banana screen can never be exact. Although some measurements were taken to reduce the disparities between the simulated particle shapes and the real ones, the diversity of particle shapes still affected the accuracy of the simulated results. Also, errors with particle size distribution were caused by the performance of the shock type-based vibrating screen. As a result, the values of screening efficiency were slightly different. However, the aim of this study was to explore the optimal screening parameters according to screening efficiency per unit time, so this was a qualitative rather than a quantitative study. The clear coincidence in trends between the DEM simulations and the experiments in Figures 9-11 demonstrates the reliability of the simulation results.

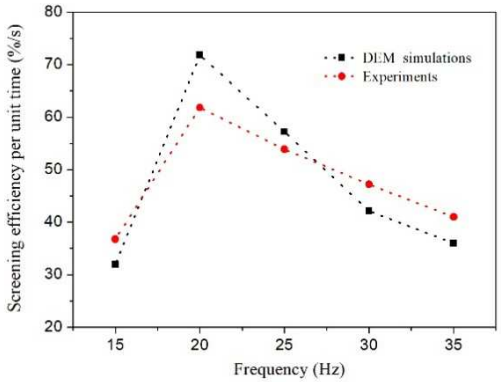


**Figure 9** Comparison of DEM simulations and experiments on frequency.

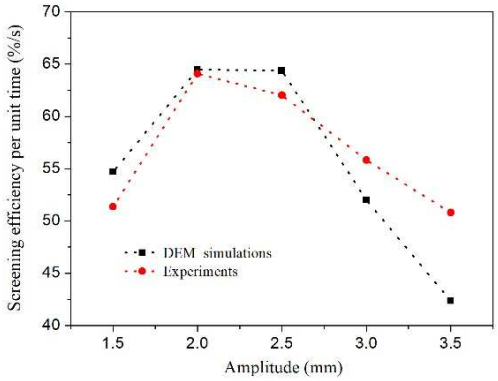


**Figure 10** Comparison of DEM simulations and experiments on amplitude.

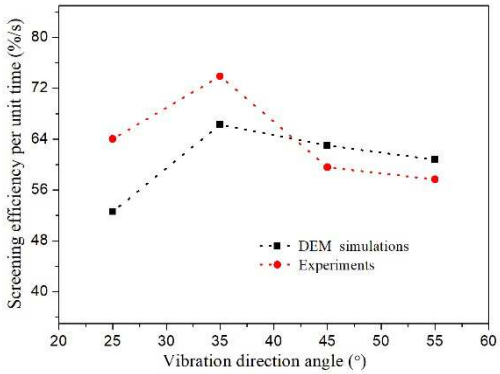


**Figure 11** Comparison of DEM simulations and experiments on vibration direction.

# 4 Orthogonal Experiment of Vibration Parameters

## 4.1 Orthogonal Experiment Scheme

In this orthogonal test, the factors frequency, amplitude and vibration direction angle (marked A, B and C) were investigated in order to find the optimal combination of vibration parameters under the highest screening efficiency. Each of the three predominant factors was segmented into four levels, as listed in Table 3. In order to ensure better sieving performance, these levels were selected according to a range near the optimal values based on the single factor experiments above. An orthogonal table of five factors and four levels was adopted.

**Table 3** Values of levels for each factor.

| Level | Frequency | Amplitude | Direction angle |
|---|---|---|---|
| 1 | 18 | 1.8 | 33 |
| 2 | 20 | 2 | 35 |
| 3 | 22 | 2.2 | 37 |
| 4 | 24 | 2.4 | 39 |

## 4.2 Orthogonal Experiment Result and Analysis

### 4.2.1 Orthogonal Design-direct Analysis

The screening efficiency per unit time under various combinations of different vibration parameter levels was obtained as shown in Table 4, where $k_i$ stands for the average of efficiency for the $i$th level of each factor. The ranges of efficiency of each level were also calculated.

Range analysis is a numerical analysis method to find out the levels of importance of each vibration factor according to the orthogonal experiment. The greater the range, the greater the change in efficiency caused by the factor in the column. Thus, the vibration parameter that holds the maximum range has the largest effect on the results of the experiment and is referred to as the main factor.

The ranges in Table 4 show that frequency had the greatest influence on screening efficiency. Amplitude takes the second place and vibration direction angle ranks third. The relationships between each factor and screening efficiency per unit time are provided in Figure 12.

**Table 4** Orthogonal experimental scheme and calculation analysis.

| Experiment | Column number | | | | | Screening efficiency per unit time (%/s) |
|---|---|---|---|---|---|---|
| | A | B | C | Blank column | Blank column | |
| 1 | 1 | 1 | 1 | 1 | 1 | 42.239 |
| 2 | 1 | 2 | 2 | 2 | 2 | 51.698 |
| 3 | 1 | 3 | 3 | 3 | 3 | 59.845 |
| 4 | 1 | 4 | 4 | 4 | 4 | 65.643 |
| 5 | 2 | 1 | 2 | 3 | 4 | 56.213 |
| 6 | 2 | 2 | 1 | 4 | 3 | 61.663 |
| 7 | 2 | 3 | 4 | 1 | 2 | 68.766 |
| 8 | 2 | 4 | 3 | 2 | 1 | 68.391 |
| 9 | 3 | 1 | 3 | 4 | 2 | 64.006 |
| 10 | 3 | 2 | 4 | 3 | 1 | 65.168 |
| 11 | 3 | 3 | 1 | 2 | 4 | 69.042 |
| 12 | 3 | 4 | 2 | 1 | 3 | 64.735 |
| 13 | 4 | 1 | 4 | 2 | 3 | 63.665 |
| 14 | 4 | 2 | 3 | 1 | 4 | 63.587 |
| 15 | 4 | 3 | 2 | 4 | 1 | 61.936 |
| 16 | 4 | 4 | 1 | 3 | 2 | 60.618 |
| $k_1$ | 54.856 | 56.531 | 58.390 | 59.832 | 59.434 | |
| $k_2$ | 63.758 | 60.529 | 58.646 | 63.199 | 61.272 | |
| $k_3$ | 65.738 | 64.897 | 63.957 | 60.461 | 62.477 | |
| $k_4$ | 62.576 | 64.847 | 65.811 | 63.312 | 63.621 | |
| range | 10.882 | 8.366 | 7.421 | 3.480 | 4.187 | |
| order of importance | | | | A > B > C | | |
| optimal solution | | | | $A_3B_3C_4$ | | |

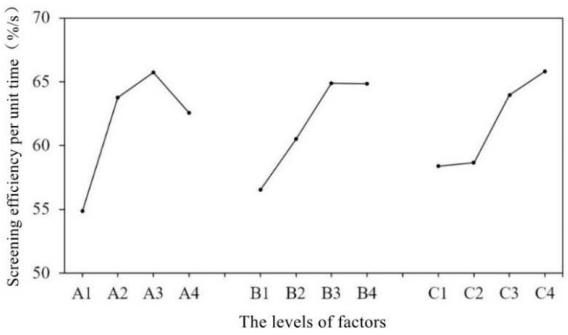


**Figure 12** Relationship chart between each factor and screening efficiency per unit time.

### 4.2.2 Orthogonal Design-variance Analysis

It is obvious that the range analysis involves a simple calculation process, however, precise values cannot be given to evaluate the magnitude of the effect of the respective factors on the experimental results. In order to cover this shortcoming of the range analysis, a variance analysis of the screening efficiency per unit time (see Table 5) was used in this work for further study.

**Table 5** Analysis of variance table.

| Factors | $SS_T$ | $df$ | $MS$ | F-value | F critical-value | Significance |
|---|---|---|---|---|---|---|
| A | 271.766 | 3 | 90.589 | 6.973 | 3.290 | ♂ |
| B | 192.867 | 3 | 64.289 | 4.949 | 3.290 | ♂ |
| C | 169.097 | 3 | 56.366 | 4.339 | 3.290 | ♂ |
| Error | 77.95 | 6 | 12.991 | | | |

In Table 4, $SS_T$ is the sum of squares of deviations, which is given by Eq. (14):

$$SS_T = \sum_{i=1}^{n}\left(y_i - \bar{y}\right)^2 = \sum_{i=1}^{n} y_i^2 - \frac{1}{n}\left(\sum_{i=1}^{n} y_i\right)^2 \tag{14}$$

where $y_i$ is the result of each orthogonal experiment and $\bar{y}$ is the average of all the simulated results. $df$ is the degree of freedom, which can be calculated by Eq. (15):

$$df = r - 1 \tag{15}$$

where $r$ is the number of levels of each factor. Additionally, the mean square of $SS_T$, which is called $MS$, is given by Eq. (16):

$$MS = \frac{SS_T}{df} \tag{16}$$

The value of $F$ in Table 4 is given by Eq. (17):

$$F = \frac{MS}{MS_e} \tag{17}$$

where $MS_e$ is the mean square of the test error. The significance of each factor for screening performance can be tested by the value of $F$. For instance, the $F$-value can check the effects of factor A on the results of the test. When a significance level $\alpha$ is given, the critical $F$-value, written as $F_\alpha(df_A, df_e)$, can be found in the $F$-distribution table. Comparing $F_A$ with $F_\alpha(df_A, df_e)$, if $F_A > F_\alpha(df_A, df_e)$ then factor A has a significant influence on the test results.

And if $F_A < F_\alpha(df_A, df_e)$ then it means that factor A has no significant impact on the results of the experiment. In this work, given $\alpha = 0.05$, the results of the *F*-value and the critical *F*-value are listed in Table 4. Additionally, the stars in Table 4 mean that the corresponding factor has a significant influence on the screening efficiency per unit time.

From the variance analysis in Table 4, it is concluded that frequency, amplitude and vibration direction angle have a significant effect on the screening efficiency per unit time of the banana screen. Therefore, the optimal combination of vibration parameters is $A_3B_3C_4$, which means that frequency is assigned the value 22 Hz, amplitude the value 2.2 mm, and direction angle the value 39°.

## 5 Conclusions

Linear vibration screening with a typical banana screen was numerically emulated by a three-dimensional DEM model. The influence of vibration parameters on screening efficiency per unit time was studied, which led to the following conclusions.

1. Empirical formulas were set up by regression analysis to elaborate the relationships between the screening efficiency per unit time and the relevant factors. When the parameters (frequency, amplitude and vibration direction angle) are extremely high or low, screening efficiency per unit time is relatively low (as shown in Figures 4-6). This means that with the increase of the values of these parameters, the screening efficiency per unit time increases first and then displays a descending trend.
2. An orthogonal experiment was performed to achieve the optimal combination of vibration parameters for maximum efficiency. The study result revealed that, based on the banana screen model, when the frequency is 22 Hz, the amplitude is 2.2 mm and the vibration direction angle is 39°, the screening efficiency per unit time reaches its maximum, which provides a theoretical basis for the parametric design of banana screens.

## Acknowledgements

The author wishes to gratefully acknowledge the support from the National Natural Science Foundation of China (51175190), Fujian Natural Science Foundation (2015J01180, 2017J01675), Key Projects of Fujian Provincial Youth Natural Fund (JZ160460), 51st Scientific Research Fund Program of Fujian University of Technology (GY-Z160139), Program for Scientific and Technological Innovation Projects of Fujian Province (2014H2002) and the

Scientific Innovation Research Foundation for Graduate Students of Huaqiao University (1511303045).

## References

[1] Standish, N., *The Kinetics of Batch Sieving*, Powder Technology, **41**(1), pp. 57-67, 1985.

[2] Xiao, J.Z. & Tong, X., *Characteristics and Efficiency of a New Vibrating Screen with a Swing Trace*, Particuology, **11**(5), pp. 601-606, 2013.

[3] Dong, K.J., Yu, A.B. & Brake, I., *DEM Simulation of Particle Flow on a Multi-deck Banana Screen*, Minerals Engineering, **22**(11), pp. 910-920, 2009.

[4] Liu, C.S., Wang, H., Zhao, Y.M., Zhao, L.L. & Dong, H.L., DEM *Simulation of Particle Flow on a Single Deck Banana Screen*, International Journal of Mining Science and Technology, **23**(2), pp. 277-281, 2013.

[5] Wang, G.F. & Tong, X., *Screening Efficiency and Screen Length of a Linear Vibrating Screen Using DEM 3D Simulation*, International Journal of Mining Science and Technology, **21**(3), pp. 451-455, 2011.

[6] Cundall, P.A. & Strack, O.D.L., *A Discrete Numerical Model for Granular Assemblies*, Geotechnique, **29**(30), pp. 331-336, 1979.

[7] Elskamp, F. & Kruggel-Emden, H., *Review and Benchmarking of Process Models for Batch Screening based on Discrete Element Simulations*, Advanced Powder Technology, **26**(3), pp. 679-697, 2015.

[8] Cleary, P.W. & Sawley, M.L., *DEM Modelling of Industrial Granular Flows: 3D Case Studies and the Effect of Particle Shape on Hopper Discharge*, Applied Mathematical Modelling, **26**(2), pp. 89-111, 2002.

[9] Xiao, J.Z. & Tong, X., *Particle Stratification and Penetration of a Linear Vibrating Screen by the Discrete Element Method*, International Journal of Mining Science and Technology, **22**(3), pp. 357-362, 2012.

[10] Zhu, H.P., Zhou, Z.Y., Yang, R.Y. & Yu, A.B., *Discrete Particle Simulation of Particulate Systems: a Review of Major Applications and Findings*, Chemical Engineering Science, **63**(23), pp. 5728-5770, 2008.

[11] Weerasekara, N.S., Powell, M.S., Cleary, P.W., Tavares, L.M., Evertsson, M., Morrison, R.D., Quist, J. & Carvalho, R.M., *The Contribution of DEM to the Science of Comminution*, Powder Technology, **248**(248), pp. 3-24, 2013.

[12] Combarros, H.J**.,** Feise, Zetzener & Kwade, *Segregation of Particulate Solids: Experiments and DEM Simulation*s, Particuology, **12**(1), pp. 25-32, 2014.

[13] Cleary, P.W. & Sinnott, M.D., *Simulation of Particle Flows and Breakage in Crushers Using DEM: Part 1 – Compression Crushers*, Minerals Engineering, **74**, pp. 178-197, 2015.

[14] Cleary, P.W., *DEM Prediction of Industrial and Geophysical Particle Flows*, Particuology, **8**(2), pp. 106-118, 2010.
[15] Xia, H.H., Tong, X., Li, Z.F. & Wu, X.Q., DEM-FEM *Coupling Simulations of the Interactions between Particles and Screen Surface of Vibrating Screen*, International Journal of Mining & Mineral Engineering, **8**(3), pp. 250, 2017.
[16] Feng, K., Montoya, B.M. & Evans, T.M., *Discrete Element Method Simulations of Bio-cemented Sands*, Computers & Geotechnics, 85, pp. 139-150, 2017.
[17] Takeuchi, S., Wang, S. & Rhodes, M., *Discrete Element Method Simulation of Three-dimensional Conical-base Spouted Beds*, Powder Technology, **184**(2), pp. 141-150, 2008.
[18] Mindlin, R.D. & Deresiewicz, H., *Elastic Spheres in Contact under Varying Oblique Forces*, Journal of Applied Mechanics-transactions of the ASME, **20**(3), pp. 327-344, 1953.
[19] Rothenburg, L. & Bathurst, R.J., *Numerical Simulation of Idealized Granular Assemblies with Plane Elliptical Particles*, Computers & Geotechnics, **11**(4), pp. 315-329, 1991.
[20] Cundall, P.A., *Formulation of a Three-dimensional Distinct Element Model – Part I. A Scheme to Detect and Represent Contacts in a System Composed of Many Polyhedral Blocks*, International Journal of Rock Mechanics & Mining Sciences & Geomechanics Abstracts, **25**(3), pp. 107-116, 1988.
[21] Hopkins, M.A., Hibler, W.D. & Flato, G.M., *On the Numerical Simulation of the Sea Ice Ridging Process*, Journal of Geophysical Research Oceans, **96**(4), pp. 4809-4820, 1991.
[22] Potapov, A.V. & Campbell, C.S*., A Three-dimensional Simulation of Brittle Solid Fracture*, International Journal of Modern Physics C, **7**(5), pp. 717-729, 1996.
[23] Elskamp, F., Kruggel-Emden, H., Hennig, M. & Teipel, U., *Benchmarking of Process Models for Continuous Screening based on Discrete Element Simulations*, Minerals Engineering, **83**(3), pp. 78-96, 2015.
[24] Li, Z.F., Tong, X., Zhou, B. & Wang, X.Y., *Modeling and Parameter Optimization for the Design of Vibrating Screens*, Minerals Engineering, **83**, pp. 149-155, 2015.